

# Measurement of the $HZ\gamma$ coupling at the future linear $e^+e^-$ collider

M. Dubinin<sup>1</sup>, H.J. Schreiber<sup>2</sup>, A. Vologdin<sup>1</sup>

<sup>1</sup> Institute of Nuclear Physics, Moscow State University, 119 992 Moscow, Russia

<sup>2</sup> DESY Zeuthen, 15735 Zeuthen, Germany

Received: 5 March 2003 / Revised version: 14 July 2003 /

Published online: 5 September 2003 – © Springer-Verlag / Società Italiana di Fisica 2003

**Abstract.** We examine the prospects for measuring the  $HZ\gamma$  coupling of a standard model-like Higgs boson with a mass between 120 and 160 GeV at the future TESLA linear  $e^+e^-$  collider, assuming an integrated luminosity of  $1 \text{ ab}^{-1}$  and a center-of-mass energy of 500 GeV. We consider the Higgs boson produced in association with  $\nu_e\bar{\nu}_e$  via the  $WW$  fusion reaction  $e^+e^- \rightarrow \nu_e\bar{\nu}_e H$ , followed by the rare decay into a  $Z$  boson and a photon,  $H \rightarrow Z\gamma$ . Accounting for all main background contributions, a precision of 27% can be achieved in unpolarized  $e^+e^-$  collisions for  $M_H = 140 \text{ GeV}$ . With appropriate initial state polarisations  $\Delta\text{BF}(H \rightarrow Z\gamma)/\text{BF}(H \rightarrow Z\gamma)$ , or the precisions on the  $H \rightarrow Z\gamma$  partial width, can be improved to 17% and provide valuable information on the  $HZ\gamma$  coupling. For  $M_H = 120$  and 160 GeV, the small significance of the signals in unpolarized collisions sets upper limits of 79% respectively 72% at 90% confidence level on the  $H \rightarrow Z\gamma$  branching fraction.

## 1 Introduction

Following the discovery of the Higgs boson, one of the main tasks of a future linear  $e^+e^-$  collider will be precise model-independent measurements of its fundamental couplings to fermions and bosons and its total width [1]. In particular, the determination of the couplings of the Higgs boson to the other fundamental particles will be a crucial test of the nature of the Higgs particle. In this respect future linear colliders will play a major role. Different colliding options with different beam polarisations combined with adjustable center-of-mass energies in a wide range and the clean environment in these machines will allow for rather precise determinations of these couplings.

A lot of detailed studies of the standard model (SM) Higgs couplings to fermions and  $W$  and  $Z$  bosons can be found in the literature [2]. These studies demonstrate the ability of a linear collider to access these couplings with a precision of a few percent. Also the trilinear Higgs self-coupling in the double Higgs production processes  $e^+e^- \rightarrow ZHH$  and  $e^+e^- \rightarrow \nu_e\bar{\nu}_e HH$  [3] are within the possibilities of experimental verification, although with substantially lower precision.

Another set of important Higgs boson couplings is represented by the effective vertices  $Hgg$ ,  $H\gamma\gamma$  and  $HZ\gamma$ . These couplings do not occur at the tree level but are induced by loop diagrams [4]. Since the Higgs interaction is proportional to particle masses, loop contributions of massive fermions do not decouple, and these vertices could therefore serve to count the number of particles which couple to the Higgs boson. The  $Hgg$  vertex can be accessed

through the  $H \rightarrow gg$  decay in  $e^+e^-$  collisions [5] or in the fusion reaction  $gg \rightarrow H$  at the LHC [6]. The  $H\gamma\gamma$  coupling can be determined either in  $e^+e^-$  and LHC- $pp$  interactions when the Higgs decays into two photons [7,8] or directly by means of the Compton back-scattering  $\gamma\gamma$  fusion process  $\gamma\gamma \rightarrow H \rightarrow X$ , with probably the best precision [9].

In this study we explore the potential of a linear  $e^+e^-$  collider to measure the  $HZ\gamma$  coupling through the rare  $H \rightarrow Z\gamma$  decay, for masses of the Higgs particle in the range 120 to 160 GeV. Within the SM, precise electroweak data provide the existence of a light Higgs boson with a mass below 193 GeV with 95% confidence level [10], with a preference for  $M_H$  close to 120 GeV. There is also a tantalising hint of a signal in the direct search in  $e^+e^- \rightarrow HZ$  at LEP2, with a lower mass limit of  $M_H \geq 114.1 \text{ GeV}$  at 95% CL [11].

The reaction which will be used to explore the branching fraction  $\text{BF}(H \rightarrow Z\gamma)$  is

$$e^+e^- \rightarrow \nu_e\bar{\nu}_e Z\gamma, \quad (1)$$

assuming a Higgs boson mass  $M_H = 120, 140$  and  $160 \text{ GeV}$ ,  $\sqrt{s} = 500 \text{ GeV}$  and an integrated luminosity of  $\mathcal{L} = 1 \text{ ab}^{-1}$ . The assumption on the center-of-mass energy is within the reach of baseline designs of linear collider projects [12–14]. We examine as an example the prospects for measuring the  $H \rightarrow Z\gamma$  branching fraction by means of the  $WW$  fusion reaction  $e^+e^- \rightarrow \nu_e\bar{\nu}_e H$ .

The statistical precision for  $\text{BF}(H \rightarrow Z\gamma)$  is mainly determined by  $\sqrt{S+B}/S$ , where  $S$  and  $B$  are respectively the number of signal and background events within

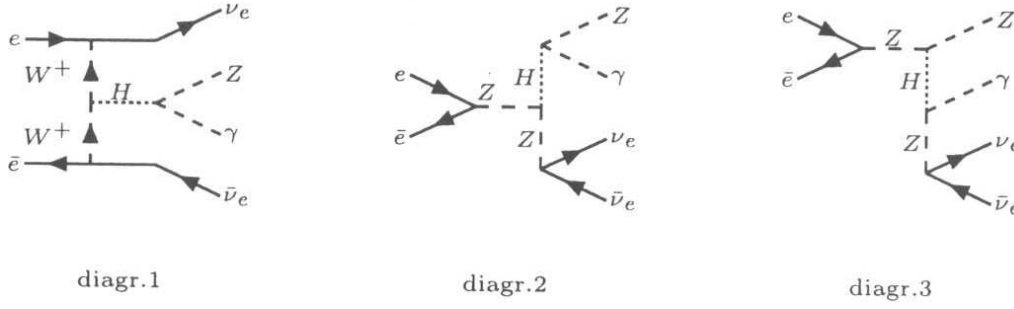


**Fig. 1.** Signal diagrams for reactions (2) and (3), with  $Z \rightarrow \nu_e \bar{\nu}_e$  and  $H \rightarrow Z\gamma$  decays

a small interval of the  $Z\gamma$  invariant mass, centered around  $M_H$ . Hence, evaluation of all relevant signal and background processes and optimization of selection procedures are mandatory, taking into account acceptances and resolutions of a linear collider detector.

Our analysis is, to our knowledge, the first on the study of  $\text{BF}(H \rightarrow Z\gamma)$  at any (future) collider. It includes the complete irreducible background and all main reducible background contributions expected. Since the SM branching fraction  $H \rightarrow Z\gamma$  is very small and there is in particular large irreducible background, the most important hadronic  $Z$  decays,  $Z \rightarrow q\bar{q}$ , are accounted for in this analysis. Although leptonic ( $e, \mu$ )  $Z$  decays provide a clean final state signature and better  $Z$  boson recognition, their rates are however too small to include them at this stage of the analysis or to allow for an independent approach.  $Z \rightarrow \nu\bar{\nu}$  decays are not considered since they prevent  $Z$  boson reconstruction in reaction (1).

This paper is organized as follows. In Sect. 2 we discuss simulation of the Higgs signal and background events and their detector response. In Sect. 3 we present the results for unpolarized  $\text{BF}(H \rightarrow Z\gamma)$  measurements. In Sect. 4 improvements to the  $H \rightarrow Z\gamma$  branching fraction measurements are discussed when e.g. beam polarisation is accounted for in signal and background events. Also, possible systematic errors and the effect of overlap with  $\gamma\gamma \rightarrow \text{hadrons}$  are reviewed. Section 5 summarizes the conclusions.

## 2 Event generation

In  $e^+e^-$  collisions the standard model Higgs boson is predominantly produced by two different processes, the Higgsstrahlung process

$$e^+e^- \rightarrow ZH, \quad (2)$$

and the weak boson ( $WW$  and  $ZZ$ ) fusion reactions

$$e^+e^- \rightarrow \nu_e \bar{\nu}_e H, \quad (3)$$

$$e^+e^- \rightarrow e^+e^- H. \quad (4)$$

The  $ZZ$  fusion process (4) is strongly suppressed with respect to the  $WW$  fusion process (3) by about a factor of 10, rather independent of  $\sqrt{s}$ . Therefore, the production channel (4) is ignored in this study. The SM tree-level

diagrams contributing to the signal reactions (2) and (3), including the  $Z \rightarrow \nu_e \bar{\nu}_e$  and  $H \rightarrow Z\gamma$  decays, are shown in Fig. 1.

In the production  $\times$  decay approximation the processes (2) and (3) are factorizable parts of the Higgs signal diagrams for the 2-to-4 body reaction (1) with electron neutrinos in the final state. In other words, the amplitude squared of diagram 1 in Fig. 1 integrated over the phase space gives  $\sigma(e^+e^- \rightarrow \nu_e \bar{\nu}_e H) \cdot \text{BF}(H \rightarrow Z\gamma)$  and the amplitudes squared of diagrams 2 and 3 give  $\sigma(e^+e^- \rightarrow ZH) \cdot \text{BF}(Z \rightarrow \nu_e \bar{\nu}_e) \cdot \text{BF}(H \rightarrow Z\gamma)$ . Thus, to be most general in our analysis, events of reaction (1) were generated for the complete set of tree-level diagrams (see Fig. 2 for the contributing background diagrams) by means of the program package CompHEP [15], including initial state bremsstrahlung and beamstrahlung for the TESLA linear collider option [16].

CompHEP performs analytic calculations of the matrix element squared, generates an optimized Fortran code and generates a flow of events. In addition, it provides for the user an appropriate kinematical scheme for the integration over the four-body phase space. The basic input parameters are taken from the report of the Particle Data Group [17] or are as listed here:  $m_b = 4.3 \text{ GeV}$ ,  $\alpha_{\text{EW}} = 1/128$ ,  $M_Z = 91.19 \text{ GeV}$ ,  $\sin^2 \theta_W = 0.23$  and  $\Gamma_Z = 2.50 \text{ GeV}$ . The CompHEP-PYTHIA interface package [18] was used to simulate the  $\nu_e \bar{\nu}_e Z\gamma \rightarrow \nu_e \bar{\nu}_e q\bar{q}\gamma$  signature. In this way, Higgs boson production and the complete irreducible background as well as possible interferences are taken into account.

For unstable particles, Breit-Wigner formulae have been used for the  $s$ -channel propagators. The Higgs boson width and the  $H \rightarrow Z\gamma$  branching fraction were imported from the program package HDECAY [19].  $\text{BF}(H \rightarrow Z\gamma)$  depends on the Higgs mass and is largest near  $M_H = 144 \text{ GeV}$ . Some values of this branching fraction, the total Higgs width and the  $HZ\gamma$  effective coupling constant relevant for our study are summarized in Table 1.

Due to the small cross-section expected for the signal reaction  $e^+e^- \rightarrow \nu_e \bar{\nu}_e H \rightarrow \nu_e \bar{\nu}_e Z\gamma$ , diagram 1 in Fig. 1, we only rely on events with the most important  $Z \rightarrow q\bar{q}$  decays. Therefore, events of process (1) are characterized by two hadronic jets originating from the  $Z$  boson, together with an energetic photon and large missing energy due to

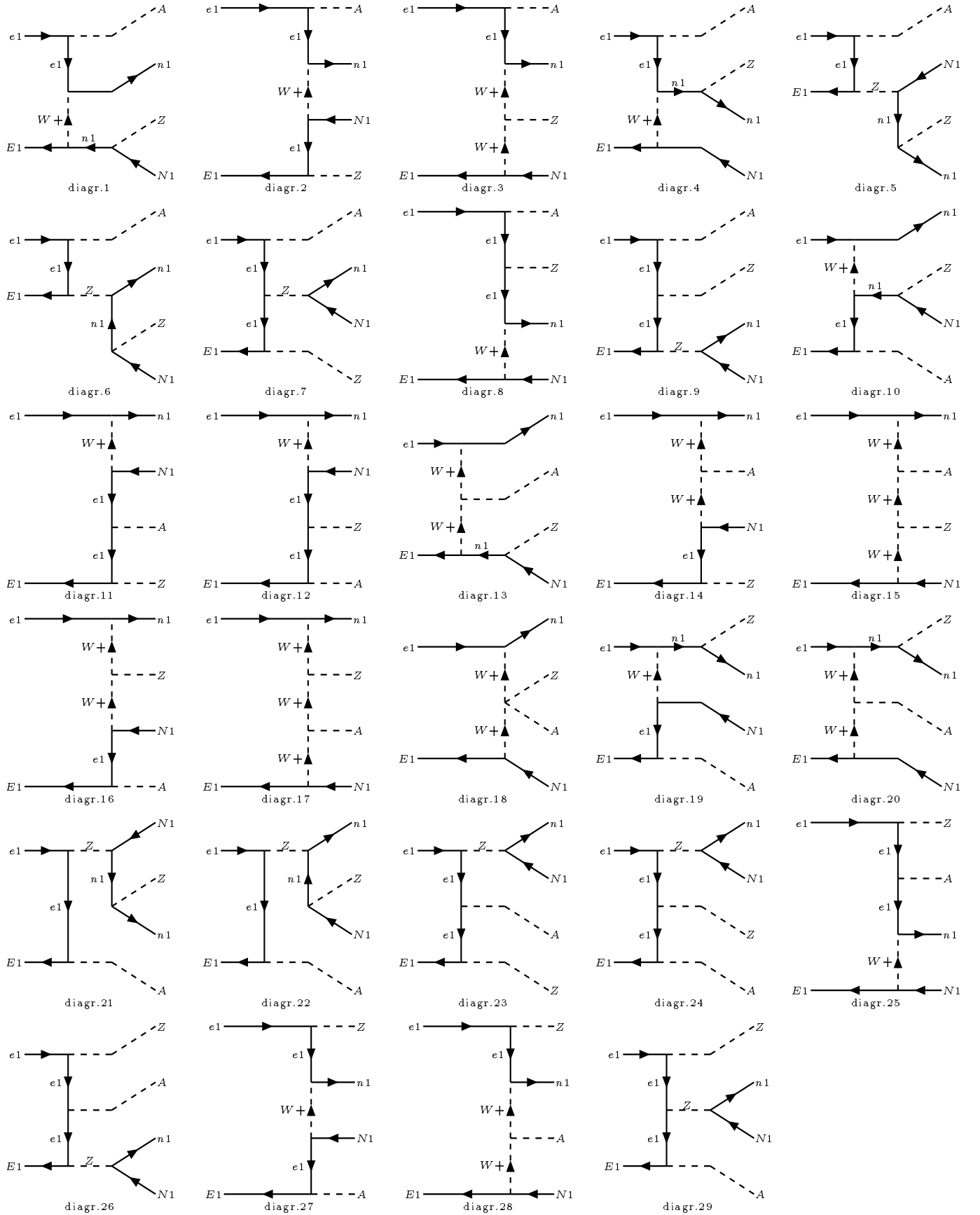


**Fig. 2.** Background diagrams for the reaction  $e^+e^- \rightarrow \nu_e \bar{\nu}_e Z \gamma$

**Table 1.** Branching fractions, total widths and effective coupling constants of the SM Higgs boson for  $M_H = 120\text{--}160$  GeV

$M_H$ , GeV	$\text{BF}(H \rightarrow Z\gamma)$	$\Gamma_{\text{tot}}$ , GeV	$\lambda_{HZ\gamma}$
120	$1.1 \cdot 10^{-3}$	$3.6 \cdot 10^{-3}$	$5.4 \cdot 10^{-5}$
140	$2.5 \cdot 10^{-3}$	$8.1 \cdot 10^{-3}$	$6.2 \cdot 10^{-5}$
160	$1.2 \cdot 10^{-3}$	$8.1 \cdot 10^{-2}$	$8.8 \cdot 10^{-5}$

the two final state neutrinos. The invariant mass of the  $Z$  and the photon should equal  $M_H$ .

The irreducible background expected from reaction (1) (the diagrams in Fig. 2) was considered at the same level as the signal events. Contributions from  $Z$  decays into  $\mu$ - and  $\tau$ -neutrinos which would occur from diagrams 7, 9, 23, 24, 26 and 29 were effectively removed by an appropriate missing mass cut (Sect. 3). Possible contributions from diagrams 5, 6, 21 and 22 with  $n_1 = N_1 = \nu_\mu$  or  $\nu_\tau$  were also calculated and found to be negligible due to large off-shell  $n_1 \rightarrow ZN_1$  decay with the  $Z$  boson close to its nominal on-shell mass value. The surviving  $\nu_\mu$  and  $\nu_\tau$  background rates were found to be smaller than 1% of the total irreducible background. An important part of the background was found to arise from the  $W$ -exchange diagrams, but significant contributions were also found to be due to the single bremsstrahlung production process  $e^+e^- \rightarrow ZZ\gamma \rightarrow \nu_e\bar{\nu}_e Z\gamma$ .

As the cross-section for the irreducible background is more than two orders of magnitude larger than the signal cross-section, we first applied the following principal cuts at the generation level, to both the signal and background events:

- (1) the photon energy should exceed 10 GeV, and
- (2) the polar angle of the photon should lie in the range 5 to 175 degrees.

After these criteria, practically all ( $\sim 96\%$ ) Higgs events survive, while the overwhelming irreducible background was substantially reduced. The cuts also largely avoid any infrared and collinear singularities in the calculation of the background amplitudes, as might be deduced from diagrams in Fig. 2.

Possible reducible backgrounds to  $e^+e^- \rightarrow \nu_e\bar{\nu}_e H$  events which might mimic the signal such as the large event rate reactions  $e^+e^- \rightarrow WW(\gamma)$ ,  $e\nu W(\gamma)$ ,  $e^+e^-(\gamma^*/Z)(\gamma)$ ,  $t\bar{t}(\gamma)$ ,  $WWZ(\gamma)$  and  $ZZZ(\gamma)$ , with beamstrahlung, initial state radiation, final state radiation and radiation from the  $W$  boson itself, were generated by either PYTHIA [20] or CompHEP [15]. The  $e^+e^- \rightarrow e\nu W(\gamma)$ ,  $e^+e^-(\gamma^*/Z)(\gamma)$  events were obtained by  $e-\gamma-e$  splitting and subsequent  $\gamma e \rightarrow \nu W$  respectively  $\gamma e \rightarrow e(\gamma^*/Z)$  interactions by PYTHIA, with proper cross-section normalizations. Only those events were used for further analyses if at least one final state photon exists with principal cut properties. It has been found that after detector response simulation and enforcing the same selection procedures as for the signal events (see below),  $t\bar{t}(\gamma)$ ,  $WWZ(\gamma)$  and  $ZZZ(\gamma)$  events were effectively discarded, also if the two  $W$  bosons from the top quarks and the prompt produced  $W$ s decay leptonically leading together with  $Z \rightarrow q\bar{q}$  to a topology similar

to the signal topology. Events from the  $e^+e^- \rightarrow WW(\gamma)$ ,  $e\nu W(\gamma)$  and  $e^+e^-(\gamma^*/Z)$  processes could however not be removed to a negligible level. Their contributions will be discussed below for the favored selection procedure.

A further potential background is expected from the process  $e^+e^- \rightarrow q\bar{q}\gamma$ , where initial state radiation and beamstrahlung reduce the center-of-mass energy available close to the Higgs mass values. Only events with a center-of-mass energy below 200 GeV, a  $q\bar{q}$  system consistent with the  $Z$  boson and a photon with large transverse energy were accepted and enforced to the selection procedures. We found that radiative return events add few non-negligible background to the final reconstructed  $Z\gamma$  mass, with some uncertainties due to the ISR model used.

Also possible contributions from the Higgs-strahlung process (2) with the dominant  $H \rightarrow b\bar{b}$  and  $WW^*$  decays were accounted for and found to contribute with four events after application of the selection procedure.

All surviving reducible background events were included in the final  $Z\gamma$  invariant mass distributions and taken into account in precision estimations for the  $H \rightarrow Z\gamma$  branching fraction.

### 3 $\text{BF}(H \rightarrow Z\gamma)$ measurements at 500 GeV

Linear collider projects reach a center-of-mass energy of 500 GeV in their baseline version [12–14]. Only in a second stage, after some years of data taking,  $\sqrt{s}$  can be extended to 0.8 or 1.0 TeV. Thus, many measurements of a possible light SM-like Higgs boson will rely on  $\sqrt{s} = 500$  GeV or less, and in combination with a large accumulated luminosity its profile will be studied in great detail.

The detector response for all generated signal and background events was simulated with the parametrized detector simulation program SIMDET\_v4 [22] using parameters as presented in the Technical Design Report [23].

Throughout this paper, it was demanded that each reconstructed event involves more than three charged particles in the final state and the total visible energy is less than 240 GeV with the transverse component relative to the beam direction below 210 GeV. Important for further analyses is the requirement that the missing mass (caused by the two undetected neutrinos) lies between 180 and 400 GeV. This cut ensures clean elimination of the Higgs-strahlung process,  $e^+e^- \rightarrow ZH \rightarrow \nu_e\bar{\nu}_e Z\gamma$ , with a missing mass close to the  $Z$  boson mass.

Large background event samples and tiny signal event rates need to pursue different strategies for extracting signal events. In a first attempt, a conventional method using simple consecutive cuts was applied to isolate Higgs signal events. Also, the generated and reconstructed events were passed through two jet cluster algorithms [20, 24], with the concern that the jet finder is able to isolate the Higgs decay photon from all other final state particles due to its distinct properties. Finally, event selection by means of the ‘‘Higgs-likeness’’ technique has been exploited where also slight differences between signal and background events are taken into account. A comparison of the selection procedures applied favors the ‘‘Higgs-likeness’’ method. The

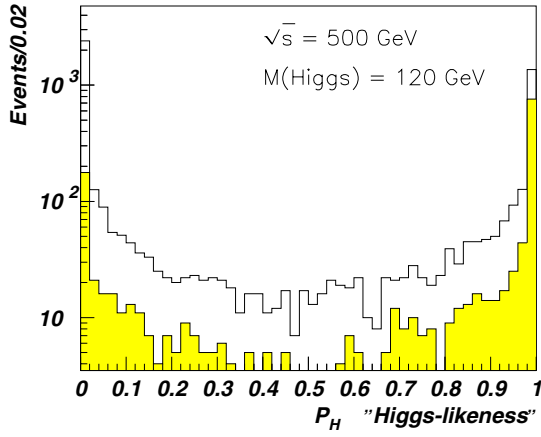


**Fig. 3.** Distribution of the discriminant variable  $P_H$  for  $e^+e^- \rightarrow \nu_e \bar{\nu}_e H \rightarrow \nu_e \bar{\nu}_e Z\gamma$  signal events (shaded histogram) and the sum of signal and background contributions

other two methods allowed for more background at similar signal event rates. Therefore, event selection by means of the “Higgs-likeness” strategy will be discussed in the following.

A “likelihood factor” was constructed giving a measure of the probability that an event is part of the signal. For any particular event, kinematical variables of the final state photon, the  $Z$  boson respectively the two jets and the missing neutrino system were combined into a global discriminant variable  $P_H$ . This quantity was constructed from a variety of normalized variables based on large statistics samples of simulated signal and background events. The variables used account for possible kinematic differences between the Higgs events (diagram 1 in Fig. 1) with the isotropic  $H \rightarrow Z\gamma$  decay and the background (diagrams of Fig. 2). In particular, the transverse momentum of the photon, its CMS scattering angle, the cosine of the polar angle of the  $Z$  boson, the photon polar and azimuthal decay angles in the Higgs rest frame, the CMS polar and azimuthal angles between the photon and the  $Z$ , the CMS photon energy, the collinearity angle between the electron beam and the photon, the coplanarity angles of the beam, the photon and the  $Z$  boson as well as the beam, the Higgs and the photon in the Higgs rest frame, the transverse masses of the photon and the missing system as well as the Higgs and the missing system were considered. In events where more than one photon candidate exists (about 48% of the cases) the photon with largest energy was selected as the Higgs decay candidate. For each event which passes the principal cuts, the event and jet quality cuts<sup>1</sup> and the fit constraint  $M_{jj} = M_Z$ , signal and background probabilities were then calculated, and by multiplication of all signal probabilities the sensitivity for an event to be a Higgs candidate was maximized. The quantity so obtained is constrained to lie in the region  $[0; 1]$ . Background events are preferably distributed at low

<sup>1</sup> For each jet we required the number of particles involved to be greater than 3, the jet energy to exceed 8 GeV, the angle between any two jets to be larger than  $20^\circ$  and the jet polar angle to be within  $|\cos \Theta_{\text{jet}}| < 0.95$ .

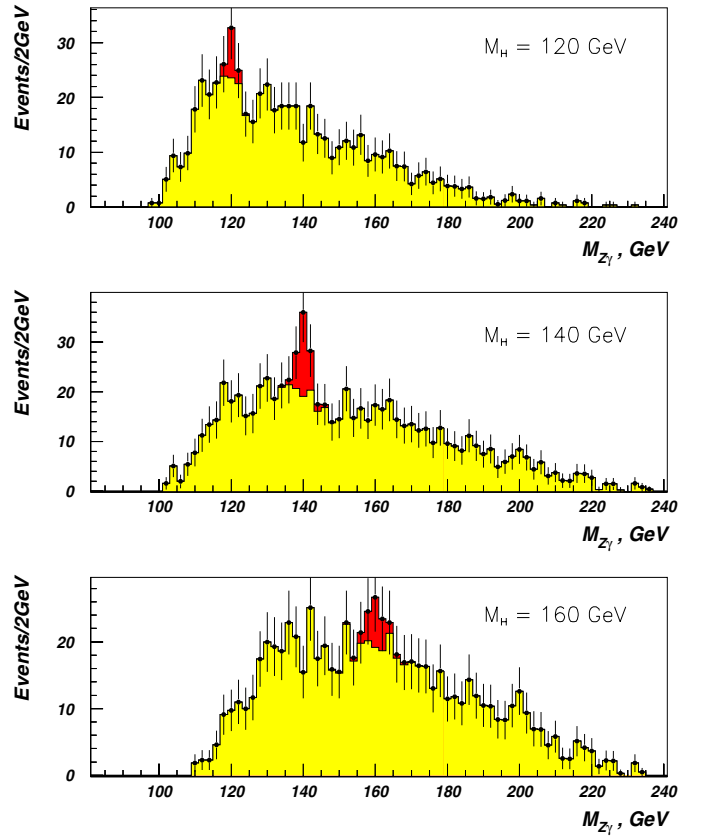


**Fig. 4.**  $M_{Z\gamma}$  invariant mass distributions for surviving signal and background events at  $\sqrt{s} = 500$  GeV, for  $M_H = 120, 140$  and  $160$  GeV and  $1 \text{ ab}^{-1}$  integrated luminosity

$P_H$  values, while for Higgs signal events  $P_H$  is close to unity. Since several variables included in the analysis vary with the Higgs mass, signal probabilities were individually determined for  $M_H = 120, 140$  and  $160$  GeV. Therefore, the “Higgs-likeness” exists for each Higgs mass considered. Figure 3 shows, as an example,  $P_H$  for  $M_H = 120$  GeV signal and the sum of signal and background events. Similar distributions were obtained for  $M_H = 140$  and  $160$  GeV. Finally, only events were retained if the energy of the Higgs photon candidate,  $\gamma_H$ , was greater than 20 GeV with the transverse component  $E_T > 15$  GeV. A reducible background was found to arise from  $WW(\gamma)$ ,  $e\nu W(\gamma)$  and radiative return events, with rates of at most 32% of the irreducible background at the 160 GeV Higgs mass.

Figure 4 shows the  $Z\gamma$  invariant mass spectra for the luminosity adjusted  $\nu_e \bar{\nu}_e Z\gamma$  signal and background events surviving the cut  $P_H > 0.98$ , for  $M_H = 120, 140$  and  $160$  GeV. For the 140 GeV case, a convincing Higgs signal is evident on a non-negligible background. Degraded event rates for the other two cases exclude reliable  $H \rightarrow Z\gamma$  branching fraction estimates. Variation of the discriminant variable  $P_H$  between 0.82 and 0.98 does not improve  $S/B$ , but would rather lower the signal-to-background ratio.

Selection efficiencies for the  $\nu_e \bar{\nu}_e Z\gamma \rightarrow \nu_e \bar{\nu}_e q\bar{q}\gamma$  signature, the number of signal ( $S$ ) and irreducible background ( $B$ ) events in the mass range  $M_{Z\gamma}$  between 117 and 123

**Table 2.** “Higgs-likeness” selection efficiencies for both signal and background  $\nu_e\bar{\nu}_eq\bar{q}\gamma$  signature, together with significances and precisions of  $\sigma(e^+e^- \rightarrow \nu_e\bar{\nu}_eH) \cdot \text{BF}(H \rightarrow Z\gamma) \cdot \text{BF}(Z \rightarrow q\bar{q})$  for  $M_H = 120, 140$  and  $160$  GeV, at the  $e^+e^-$  linear collider with  $\sqrt{s} = 500$  GeV. A total integrated luminosity of  $1 \text{ ab}^{-1}$  is assumed

	Signal	(Background)	
	$M_H = 120 \text{ GeV}$	$140 \text{ GeV}$	$160 \text{ GeV}$
Selection efficiency (%)	17.4 (0.23)	13.9 (0.20)	15.9 (0.16)
Number of events/ $1 \text{ ab}^{-1}$	16 (51)	29 (44)	16 (41)
Significance $S/\sqrt{B}$	2.24	4.37	2.50
Precision $\sqrt{S+B}/S$	0.51	0.29	0.47

(137–143, 157–163) GeV, the significances  $S/\sqrt{B}$  and the statistical precisions  $\sqrt{S+B}/S$  obtained on  $\sigma(e^+e^- \rightarrow \nu_e\bar{\nu}_eH) \cdot \text{BF}(H \rightarrow Z\gamma) \cdot \text{BF}(Z \rightarrow q\bar{q})$  are presented in Table 2.

Accounting for all  $Z$  decays and the surviving reducible background the relative precision on the  $H \rightarrow Z\gamma$  branching fraction for  $M_H = 140$  GeV is then deduced after convolution with the uncertainty of the inclusive  $\nu_e\bar{\nu}_eH$  production rates [23]:  $\Delta\text{BF}(H \rightarrow Z\gamma)/\text{BF}(H \rightarrow Z\gamma) = 27\%$ , assuming  $1 \text{ ab}^{-1}$  integrated luminosity at  $\sqrt{s} = 500$  GeV. The small signal significances  $S/\sqrt{B}$  for the 120 and 160 GeV Higgs cases set upper limits of 79% respectively 72% at 90% confidence level for the  $H \rightarrow Z\gamma$  branching fraction.

## 4 Discussion of the results

The selection procedures applied favor the “Higgs-likeness” method, in particular for the 140 GeV Higgs mass case. We would register about 30  $H \rightarrow Z\gamma$  events in reaction (3) and some 60 total background events in the window  $M_H \pm 3 \text{ GeV}$  at  $\sqrt{s} = 500$  GeV for an integrated luminosity of  $1 \text{ ab}^{-1}$ . We regard these numbers as rather encouraging, especially considering the initial value of the  $S/B$  rate. Although a complete optimization for neither selection technique has not been achieved, we are confident that room for improved  $H \rightarrow Z\gamma$  branching fraction measurements is limited, mainly due to the presence of overwhelming irreducible background with final state signature similar to the signal events.

Higgs-strahlung events would provide an independent  $H \rightarrow Z\gamma$  branching fraction. Relying on events of reaction (1) the event rate for  $e^+e^- \rightarrow HZ$  is about a fifth of the  $WW$  fusion rate and the corresponding irreducible background is estimated to be about two times larger. If  $e^+e^- \rightarrow HZ \rightarrow (Z\gamma)Z \rightarrow (q\bar{q}\gamma)(q\bar{q})$  events with four jets in the final state are also accounted for, improvements expected on  $\Delta\text{BF}(H \rightarrow Z\gamma)/\text{BF}(H \rightarrow Z\gamma)$  are limited due to a large irreducible four-jet  $\gamma$  background and more complicated selection procedures when both  $Z$  bosons decay hadronically. In combination with the  $WW$  fusion channel the  $H \rightarrow Z\gamma$  branching fraction is anticipated to be improved by  $\sim 10\%$ .

For  $M_H = 120$  and  $160$  GeV and  $1 \text{ ab}^{-1}$  integrated luminosity, unpolarized  $e^+e^-$  collisions do not give  $H \rightarrow$

$Z\gamma$  signal significances in excess of  $3.0\sigma$ . A more favorable signal-to-background ratio should be achievable at higher energies, e.g. at  $\sqrt{s} = 1.0 \text{ TeV}$ , where the fusion cross-section is typically three times larger. However, the dominant background in process (1) scales in approximately the same way with  $\sqrt{s}$  as the signal process, as verified by CompHEP simulations. Hence, assuming (conservatively) similar surviving reducible backgrounds and selection efficiencies as at 500 GeV improved significances  $S/\sqrt{B}$  of about 3.5 (7.2, 4.4) are expected for  $M_H = 120$  (140, 160) GeV, so that access to the  $H \rightarrow Z\gamma$  branching fraction seems possible for all Higgs masses considered. Such an energy increase is however only expected at the second stage of linear collider projects [12–14], after some years of data taking at  $\sqrt{s} \leq 500$  GeV.

An alternative approach relies on studying the Higgs-strahlung process  $e^+e^- \rightarrow HZ \rightarrow ZZ\gamma$  at optimized lower energies, e.g. at  $\sqrt{s} = 300$  GeV. Considering four-jet events with a prompt photon, preliminary analyses [21, 25] indicate less precision for  $\text{BF}(H \rightarrow Z\gamma)$ .

Linear  $e^+e^-$  colliders offer the possibility for longitudinal polarized electron and positron beams, with varying polarisation degrees in right-handed or left-handed modes. The Higgs boson production rates in both processes (2) and (3) depend strongly on the polarisation degree and the helicity of the incoming particles. For any given process, the ratios of the cross-section for given electron and positron beam polarisations divided by the cross-section for unpolarized beams, denoted as  $R$ , are presented in Table 2 of [7]. The Higgs event rates in the processes (2) and (3) are enhanced most for left-handed  $e^-$  colliding with right-handed  $e^+$  with as large a degree of polarisation as possible. For the feasible though ambitious case of collisions between an  $e^-$  beam with polarisation  $P_- = -0.8$  and an  $e^+$  beam with polarisation  $P_+ = +0.6$ ,  $R = 2.88$  for the  $WW$  fusion process. However, the dominant irreducible background scales in approximately the same way with beam polarisations as the signal processes [7], the precision of the  $H \rightarrow Z\gamma$  branching fraction improves by only a factor  $\sqrt{R}$ . Under such circumstances, the relative uncertainties on  $\text{BF}(H \rightarrow Z\gamma)$  is lowered to 17% for  $M_H = 140$  GeV. Furthermore, the significances  $S/\sqrt{B}$  for  $M_H = 120$  and  $160$  GeV can be considerably increased by choosing maximally possible  $e^-$  and  $e^+$  polarisation, so that  $H \rightarrow Z\gamma$  branching fraction measurements become

feasible. However, it should be noted that other physics processes will demand different beam polarisations and the assumption of using the full luminosity with the desired beam polarisation for this particular measurement gives some lower bound to the attainable precision.

Since the signal-to-background ratio is expected to be less than unity, it should be emphasized that large continuum  $Z\gamma$  production and copious  $\pi^0$  background events must be rejected by excellent geometrical resolution and stringent isolation criteria combined with excellent electromagnetic and hadronic energy resolution and hermiticity. A worse resolution would flatten the marginal signal events over a large  $Z\gamma$  background, thus degrading the visibility of the signal. Systematic uncertainties due to detector effects such as photon detection efficiency, energy scales and resolutions are believed to be small and can be estimated from comparison of data with well understood processes, such as  $e^+e^- \rightarrow \gamma\gamma$ , Compton scattering, Bhabha,  $ZZ$  and  $WW$  events. Systematic uncertainties on the integrated luminosity are expected to be below 0.5%, and statistical uncertainties due to final simulation sample sizes should be kept below a few percent. Simulations of the standard model background channels are expected to yield most of the systematic uncertainties. The use of different event generators would keep this uncertainty under control and agreement between them within few percent is expected. Taking all these effects together and accounting for a precise measurement of the inclusive Higgs cross-section of about 4% or less [12], the error on  $\text{BF}(H \rightarrow Z\gamma)$  will be dominated by the statistical uncertainty.

The effect of overlap of  $\gamma\gamma \rightarrow \text{hadrons}$  to  $\nu_e\bar{\nu}_e H$  events has also been studied. The  $\gamma\gamma$  events due to photons radiated in the electro-magnetic interactions of the colliding beams have been generated by the GUINEA PIG program [26] with a rate modelled in [27]. PYTHIA [20] has been used to generate the hadrons. The detector simulation program SIMDET [22] overlays the  $\gamma\gamma$  events to  $e^+e^- \rightarrow \nu_e\bar{\nu}_e H$  events, and all final state particles are then reconstructed. Without special care to isolate the particles from  $\gamma\gamma$  interactions, we found that the Higgs events were recognized without notable loss or distortions after passing the selection procedure.

## 5 Conclusions

We have examined the prospects at a future linear  $e^+e^-$  collider of measuring the branching fraction of a standard model-like Higgs boson into the  $Z$  boson and a photon,  $\text{BF}(H \rightarrow Z\gamma)$ . Higgs boson masses of 120, 140 and 160 GeV and an integrated luminosity of  $\mathcal{L} = 1 \text{ ab}^{-1}$  at  $\sqrt{s} = 500 \text{ GeV}$  were assumed. In order to estimate the precision on  $\text{BF}(H \rightarrow Z\gamma)$  which can be attained, all expected background processes were included in the analysis, and acceptances and resolutions of a linear collider detector were taken into account. In particular, by simulating the 2-to-4 particle reactions  $e^+e^- \rightarrow \nu_e\bar{\nu}_e Z\gamma$ , in which the signal reaction  $e^+e^- \rightarrow \nu_e\bar{\nu}_e H$  is embedded, the complete irreducible background has been taken into account. Only  $Z \rightarrow q\bar{q}$  decays were included.

Since reactions like  $e^+e^- \rightarrow \nu_e\bar{\nu}_e Z\gamma, WW(\gamma), e\nu W(\gamma), e^+e^-(\gamma^*/Z)$  and radiative return  $q\bar{q}\gamma$  events also constitute a potentially serious background sources for the  $e^+e^- \rightarrow \nu_e\bar{\nu}_e H$  signal, different selection techniques (consecutive cuts, jet finders, “Higgs-likeness”) were applied. As the favored selection procedure the “Higgs-likeness” technique has been found.

For unpolarized beams, the expected relative precision for the  $H \rightarrow Z\gamma$  branching fraction was found to be 27% for  $M_H = 140 \text{ GeV}$ , after accounting for all  $Z$  decays and convolution with the uncertainty on the inclusive  $WW$  fusion Higgs boson cross-section. For the other two Higgs mass cases, no statistically significant excess over the backgrounds was observed. Hence, only upper limits of 79% and 72% at 90% confidence level could be deduced on  $\text{BF}(H \rightarrow Z\gamma)$ .

For an  $e^-$  beam polarisation of  $-0.8$  and a  $e^+$  beam polarisation of  $+0.6$ , the  $WW$  fusion cross-section  $\sigma(e^+e^- \rightarrow \nu_e\bar{\nu}_e H)$  is significantly enhanced, so improving substantially the precision on  $\text{BF}(H \rightarrow Z\gamma)$  to 17%, even taking into account the fact that the dominant irreducible background scales in the same way. With these uncertainties it should be possible to measure a relative precision for the  $H \rightarrow Z\gamma$  partial width of  $\frac{\Delta\Gamma(H \rightarrow Z\gamma)}{\Gamma(H \rightarrow Z\gamma)} \simeq 18\%$ , if an uncertainty of 5% for the total Higgs width [12] is included. This in turn allows one to expect a relative precision for the  $HZ\gamma$  coupling of 9% for  $M_H = 140 \text{ GeV}$ . Large data samples with the maximally possible  $e^-$  and  $e^+$  polarisation would also allow one to access the  $H \rightarrow Z\gamma$  partial width for  $M_H = 120$  and  $160 \text{ GeV}$ .

Overlap of  $\gamma\gamma \rightarrow \text{hadrons}$  to  $\nu_e\bar{\nu}_e H$  events due to photons radiated in the electro-magnetic interactions of the colliding beams would not alter the uncertainties reachable.

The results presented also suggest that the  $WW$  fusion reaction  $e^+e^- \rightarrow \nu_e\bar{\nu}_e H$  at 500 GeV would be superior in  $H \rightarrow Z\gamma$  branching fraction measurements to the Higgsstrahlung process  $e^+e^- \rightarrow HZ$  at lower energies, e.g. at  $\sqrt{s} = 300 \text{ GeV}$  [21, 25], in particular, if polarized beams are taken into account.

For Higgs masses significantly above 160 GeV, it will be difficult to determine the  $HZ\gamma$  coupling with valuable precision since the  $H \rightarrow Z\gamma$  branching fraction is too small to be accurately measured.

The linear collider will be able to accurately measure the loop induced  $H \rightarrow gg$  decay in  $e^+e^-$  collisions and the effective  $H\gamma\gamma$  coupling in  $\gamma\gamma$  collisions. Access to the loop induced  $H \rightarrow Z\gamma$  decay is more difficult or even precluded, in particular if the Higgs boson does not weigh about 140 GeV.

A more favorable signal-to-background ratio should be achieved at higher energies, e.g. at  $\sqrt{s} = 1 \text{ TeV}$ . Assuming similar selection efficiencies and  $\mathcal{L} = 1 \text{ ab}^{-1}$ , improved  $S/\sqrt{B}$  values are attainable and  $H \rightarrow Z\gamma$  branching fraction measurements appear feasible for all Higgs masses considered.

*Acknowledgements.* We would like to thank K. Desch and E. Boos for useful discussions. The work of M.D. was partially

supported by RFBR grant 01-02-1670 and INTAS grants 00-00313, 00-00679.

## References

1. See e.g. E. Accomando et al., Phys. Rep. **299**, 1 (1998)
2. For a review, see e.g. K. Desch, M. Battaglia, in Physics and experiments with future linear  $e^+e^-$  colliders, Proceedings of the 5th International Linear Collider Workshop, Batavia, IL, USA, 2000
3. G. Gounaris, D. Schildknecht, F. Renard, Phys. Lett. B **83**, 191 (1979); B **89**, 437 (1980); V. Barger, T. Han, Mod. Phys. Lett. A **5**, 667 (1990); A. Djouadi, H.E. Haber, P.M. Zerwas, Phys. Lett. B **375**, 203 (1996); V. Ilyin et al., KEK CP-030; F. Boudjema, E. Chopin, Report ENSLAPP-A534/95; D.J. Miller, S. Moretti, Eur. Phys. J. C **13**, 459 (2000); C. Castanier et al., LC-PHSM-2000-061
4. J. Ellis, M.K. Gaillard, D.V. Nanopoulos, Nucl. Phys. B **106**, 292 (1976); A.I. Vainshtein et al., Sov. J. Nucl. Phys. **30**, 711 (1979); R.N. Cahn, M.S. Chanowitz, N. Fleishon, Phys. Lett. B **82**, 113 (1979); L. Bergstrom, G. Hulth, Nucl. Phys. B **259**, 137 (1985); A. Barroso, J. Pulido, J.C. Romao, Nucl. Phys. B **267**, 509 (1986)
5. M. Battaglia, Proceedings of the Worldwide Study on Physics and Experiments with Future Linear  $e^+e^-$  Colliders, Sitges, Barcelona, Spain, April 28–May 5, 1999
6. H.M. Georgi et al., Phys. Rev. Lett. **40**, 692 (1978); A. Djouadi, M. Spira, P.M. Zerwas, Phys. Lett. B **264**, 440 (1991); S. Dawson, Nucl. Phys. B **359**, 283 (1999); M. Spira et al., Nucl. Phys. B **453**, 17 (1995)
7. E. Boos et al., Eur. Phys. J. C **19**, 455 (2001)
8. ATLAS Collaboration, ATLAS detector and physics performance, technical design report, vol. 2, report CERN/LHCC 99-15 ATLAS-TDR-15; CMS Collaboration, CMS: The electromagnetic calorimeter, technical design report, report CERN/LHCC 97-33, CMS-TDR-4
9. G. Jikia, S. Söldner-Rembold, Nucl. Phys. Proc. Suppl. **82**, 373 (2000); G. Jikia, S. Söldner-Rembold, LC-PHSM-2001-060; M. Melles, W.J. Stirling, V.A. Khoze, Phys. Rev. D **61**, 54015 (2000)
10. See e.g. G. Degrassi, hep-ph/0102137; J. Erler, hep-ph/0102143; D. Abbaneo et al. [LEP Electroweak Working Group], A. Chou et al. [SLD Heavy Flavour and Electroweak Groups], LEPEWWG/2002-01 (May 2002), and additional updates at <http://lepewwg.web.cern.ch/LEPEWWG/>
11. ALEPH Collaboration, R. Barate et al., Phys. Lett. B **495**, 1 (2000); DELPHI Collaboration, P. Abreu et al., Phys. Lett. B **499**, 23 (2001); L3 Collaboration, M. Acciari et al., Phys. Lett. B **508**, 225 (2001); OPAL Collaboration, G. Abbiendi et al., Phys. Lett. B **499**, 38 (2001); The LEP Working Group for Higgs Boson Searches, hep-ex/0107029; LHWG Note 2002-01 (July 2002), and additional updates at <http://lephiggs.web.cern.ch/LEPHIGGS/www/Welcome.html>
12. TESLA Technical Design Report, DESY 2001-011, ECFA 2001-209, hep-ph/0106315, March 2001
13. American Linear Collider Working Group, BNL-67545, FERMILAB-Pub-00/152, LBNL-46299, SLAC-PUB-8495, UCRL-ID-139524, July, 2000
14. ACFA Linear Collider Working Group Report, KEK Report 2001-11, hep-ph/0109166, September 2001
15. E.E. Boos et al., INP MSU 94-36/358 and SNUTP-94-116, hep-ph/9503280; P. Baikov et al., Proceedings of the Xth Int. Workshop on High Energy Physics and Quantum Field Theory, QFTHEP-95, edited by B. Levtchenko, V. Savrin, Moscow, 1995, p. 101; A. Pukhov et al., CompHEP user's manual, v.3.3, INP MSU 98-41.542; hep-ph/9908288
16. D. Schulte, private communication; T. Ohl, IKDA 96/13-rev., July 1996 and hep-ph/9607454-rev
17. D.E. Groom et al., Eur. Phys. J. C **15**, 1 (2000)
18. A.S. Belyaev et al., hep-ph/0101232
19. A. Djouadi, J. Kalinowski, M. Spira, Comput. Phys. Commun. **108**, 56 (1998)
20. T. Sjöstrand, Comput. Phys. Commun. **82**, 74 (1994); hep-ph/0001032; T. Sjöstrand et al., Comput. Phys. Commun. **135**, 238 (2001)
21. M. Dubinin, H.J. Schreiber, A. Vologdin, in preparation
22. M. Pohl, H.J. Schreiber, DESY 02-061, May 2002, hep-ex/0206009, LC-DET-2002-005
23. TESLA Technical Design Report, Part IV, A Detector for TESLA, DESY 2001-011, ECFA 2001-209, hep-ph/0106315, March 2001
24. S. Bethke et al., Nucl. Phys. B **370**, 310 (1992)
25. T. Cubitt, DESY Zeuthen summer student write-up, October 2001
26. D. Schulte, TESLA note 97-08
27. G.A. Schuler, T. Sjöstrand, CERN-TH/96-119